CP VIOLATION STUDIES IN B DECAYS WITH LHCB

YUEHONG XIE (on behalf of the LHCb Collaboration)
School of Physics and Astronomy, University of Edinburgh, Edinburgh EH9 3JZ, UK

Search for new physics beyond the Standard Model through study of CP violation (CPV) using B meson decays is one of the major physics goals of the LHCb experiment. In this contribution, first results of CPV studies using data collected in the 2010 LHC run are presented. Results, status and prospects of the analysis of the golden decay channel $B_s \to J/\psi\phi$ are discussed in detail. Also presented are the first observations of the $B_s \to J/\psi f_0$ and $B_s \to K^{*0}\bar{K}^{*0}$ decays, both of which will be used to probe CP violating new physics at LHCb. Future prospects of CPV studies in B decays at LHCb are discussed.

1 Why Study CP Violation at LHCb

The major physics objective of the LHCb experiment is to search for effects of new physics (NP) beyond the Standard Model (SM) in loop-mediated processes. The study of CP violation (CPV) is a powerful tool to search for NP. In the SM, CPV originates from a complex phase in the CKM matrix. Any departure of a CPV measurement from its SM prediction is a signal of NP. Particularly interesting places to search for NP are loop processes, where NP contribution could significantly modify the SM predictions. LHCb aims to perform high precision studies of CPV using many different decay processes of B mesons, particularly B_s mesons. [1] For instance, $B_s \to J/\psi\phi$ and $B_s \to J/\psi f_0$ decays can be used to probe NP contributions to B_s mixing via box diagrams; $B_s \to K^{*0}\bar{K}^{*0}$, $B_s \to \phi\phi$ and $B_s \to K^+K^-$ decays can be used to probe NP contributions in decay processes via loop diagrams.

2 The LHCb Detector and 2010 Data Sample

The LHCb detector is a single arm forward spectrometer, described in detail elsewhere. [2] The features essential for CPV study include: precise vertexing and tracking; good particle identification; efficient and flexible trigger. The data sample used to obtain the reported results corresponds to an integrated luminosity of about 36 pb^{-1} and was collected at an centre-of-mass energy of $\sqrt{s} = 7$ TeV in the 2010 LHC run.

3 Analysis of $B_s \to J/\psi\phi$ and related channels

$B_s \to J/\psi\phi$ is a golden decay channel for CPV study. In the SM, the weak phase difference between the amplitudes of direct decay and decay via mixing is clearly predicted to be $\phi_s = -2\beta_s$, where $\beta_s = \arg\left(-V_{ts}V_{tb}^*/V_{cs}V_{cb}^*\right)$. An indirect determination via global fits to experimental data gives $2\beta_s = (0.0363 \pm 0.0017)$ rad. [3] However, NP contributions to B_s mixing can significantly alter this expectation. Besides the weak phase, the difference between the decay width of the light and heavy mass eigenstates of the B_s system, $\Delta\Gamma_s$, is also of theoretical interest.

The measurement of ϕ_s and $\Delta\Gamma_s$ in $B_s \to J/\psi\phi$ requires a complicated flavour-tagged time-dependent angular analysis. This section discusses the analysis of not only $B_s \to J/\psi\phi$, but also some related channels used to validate the analysis procedure and demonstrate our good understanding of the detector effects such as background, resolution, acceptance and wrong tag probability.

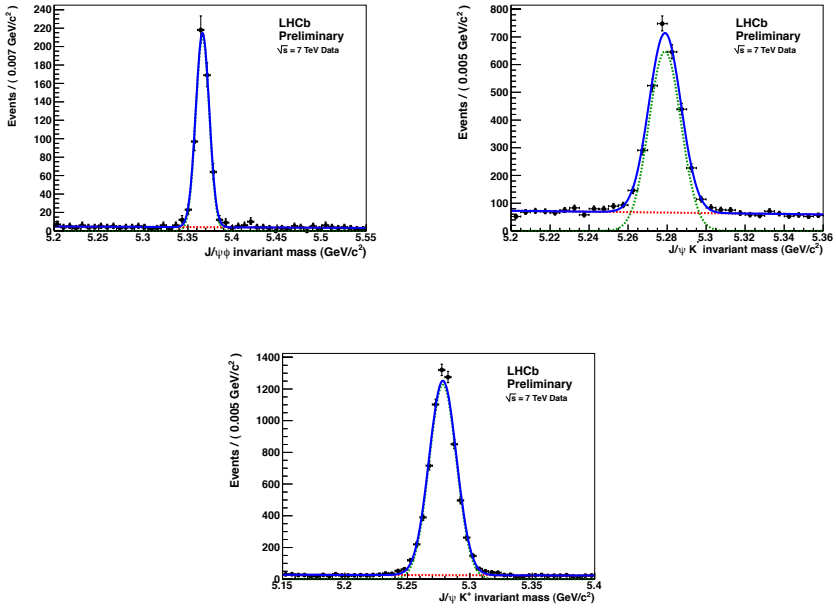

Figure 1: $B_s \to J/\psi\phi$ (top left), $B^0 \to J/\psi K^*$ (top right) and $B^+ \to J/\psi K^+$ (bottom) mass distributions with $t > 0.3$ ps. Superimposed are the total fit (solid blud), signal projection modeled by a single Gaussian (dashed green) and background projection modeled by a linear function (dashed red).

3.1 Selection of $b \to J/\psi X$ Channels

Five $b \to J/\psi X$ channels ($B_s \to J/\psi\phi$, $B^0 \to J/\psi K^{*0}$, $B^+ \to J/\psi K^+$, $B^0 \to J/\psi K^0_S$ and $\lambda_b \to J/\psi\Lambda$) are triggered and selected using similar criteria wherever possible. The baseline selection minimizes the distortion of proper time distributions in order to reduce the systematic uncertainties for time-dependent analysis. This selection retains the prompt background events with proper time $t \sim 0$, from which the proper time resolution is estimated to be $\sigma_t \approx 50$ fs. The reconstructed B mass resolution is excellent, ranging from 6 to 11 MeV for the various modes. The background level is found to be very low for $t > 0.3$ ps, as shown in Figure 1.

3.2 Lifetime Measurements in $b \to J/\psi X$ Channels

A maximum likelihood fit is performed to the proper time distribution of fully reconstructed candidates in the range $t \in [0.3, 14]$ ps in each decay mode. In the fit the theoretical proper time distribution of the signal events is modeled by a single exponential function. This ignores the non-zero decay-width difference of the B_s system. The extracted lifetimes and signal yields are given in Table 1. Details can be found in the reference [4].

Table 1: Signal event yields and lifetimes extracted from the likelihood fits to the candidate time distributions.

Channel	Lifetime (ps)	Yield
$B^+ \to J/\psi K^+$	1.689 ± 0.022 (stat.) ± 0.047 (syst.)	6741 ± 85
$B^0 \to J/\psi K^{*0}$	1.512 ± 0.032 (stat.) ± 0.042 (syst.)	2668 ± 58
$B^0 \to J/\psi K_S$	1.558 ± 0.056 (stat.) ± 0.022 (syst.)	838 ± 31
$B_s \to J/\psi\phi$	1.447 ± 0.064 (stat.) ± 0.056 (syst.)	570 ± 24
$\Lambda_b \to J/\psi\Lambda$	1.353 ± 0.108 (stat.) ± 0.035 (syst.)	187 ± 16

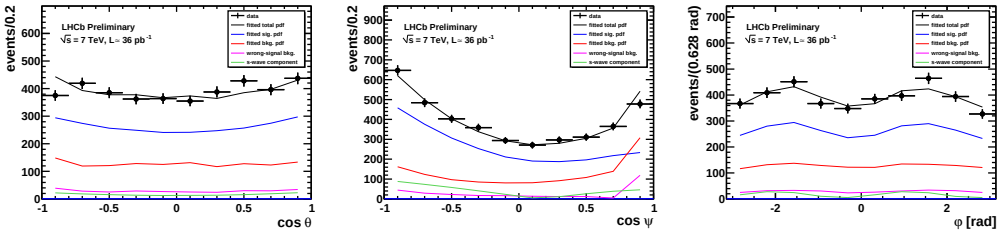

Figure 2: The transversity angle distributions for the selected $B^0 \to J/\psi K^*$ candidates, compared to the total fit (black solid), the projections for signal (blue), S-wave (green), total background (red) and wrong-signal (purple).

3.3 Angular Analysis of $B^0 \to J/\psi K^{*0}$

Both $B_s \to J/\psi\phi$ and $B^0 \to J/\psi K^*$ are decays of a pseudo-scalar meson into two vector mesons. A maximum likelihood fit to the angular distribution is needed to extract the polarization amplitudes and strong phases. A detailed description of the fit technique is in the reference [5]. The results extracted from a fit to the $B^0 \to J/\psi K^*$ decays are given in Table 2. The fit includes an S-wave contribution. The distributions of the transversity angular variables, which are defined in the reference [5], are shown in Figure 2.

Table 2: Results of a fit to the selected $B^0 \to J/\psi K^{*0}$ events, and comparison with Babar results. The first and second errors are statistical and systematic, respectively.

Parameter	LHCb results	Babar results [6]
$\|A_{\|\|}\|^2$	0.252 ± 0.020 ± 0.016	0.211 ± 0.010 ± 0.006
$\|A_\perp\|^2$	0.178 ± 0.020 ± 0.016	0.233 ± 0.010 ± 0.005
$\delta_{\|\|}$ (rad)	-2.87 ± 0.11 ± 0.010	-2.93 ± 0.08 ± 0.004
$\delta_\perp$ (rad)	3.02 ± 0.010 ± 0.07	2.91 ± 0.05 ± 0.003

3.4 Untagged Time-dependent Angular Analysis of $B_s \to J/\psi\phi$

A maximum likelihood fit is performed to the 4-dimensional time and angular distribution. In addition to the polarization magnitudes and strong phases, the probability density function involves also the weak phase ϕ_s, the B_s average decay width Γ_s and the decay width difference $\Delta\Gamma_s$. Since no tagging information is used in this analysis, the data has very little power to constrain ϕ_s. The fit results when fixing $\phi_s = 0$ is given in Table 3. Fits without fixing ϕ_s are also performed. The confidence contours in the ($\Delta\Gamma_s$, ϕ_s) plane derived using the Feldman-Cousins method [8] is shown in Figure 3. Details can be found in the reference [5].

Table 3: Results of a fit to the selected $B_s \to J/\psi\phi$ candidates with $\phi_s = 0$ fixed in the fit. The first and second errors are statistical and systematic, respectively.

Parameter	LHCb results	CDF results [7]
Γ_s	0.679 ± 0.036 ± 0.027	0.653 ± 0.011± 0.005
$\Delta\Gamma_s$	0.077 ± 0.119 ± 0.021	0.075 ± 0.035 ± 0.010
$\|A_0\|^2$	0.528 ± 0.040 ± 0.028	0.524 ± 0.013 ± 0.015
$\|A_\perp\|^2$	0.263 ± 0.056 ± 0.014	/
$\delta_{\|\|}$ (rad)	3.14 ± 0.52 ± 0.013	/

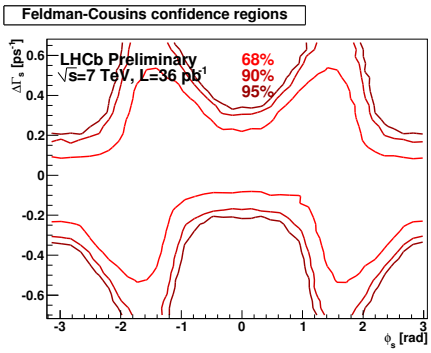

Figure 3: The confidence contours in the ($\Delta\Gamma_s$, ϕ_s) plane from untagged fits to $B_s \to J/\psi\phi$ candidates.

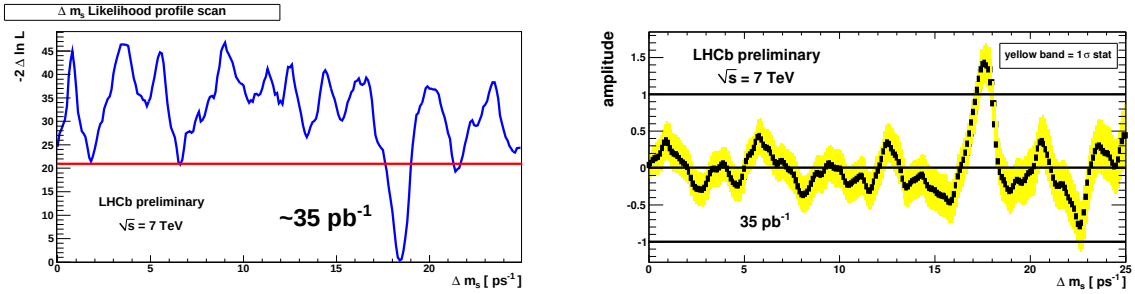

Figure 4: Left: likelihood scan for Δm_s; Right: fitted amplitude as a function of Δm_s.

3.5 Flavour Tagging and Measurements of Δm_s and Δm_d

The initial flavour of a B particle can be inferred from the products of the other B particle (called "opposite side tagging"), or from the fragmentation particles associated to the production of the signal B particle (called "same side tagging"). Currently the same side tagging is still under development. The opposite side tagging software is optimized and calibrated using control channels $B^0 \to D^{*-}\mu^+\nu_\mu$, $B^+ \to J/\psi K^+$ and $B^0 \to J/\psi K^{*0}$. More details about flavour tagging performance are given in the reference [9]. The flavour tagging software is validated in the measurements of Δm_s and Δm_d.

About 1350 B_s signals are reconstructed in the $B_s \to D_s^-(3)\pi$ decays. Using opposite side tagging information a 4.6 σ significant mixing signal is observed and the mixing frequency is measured to be $\Delta m_s = 17.63 \pm 0.11$ (stat.) $\pm$ 0.04 (syst.) ps^{-1}, [10] in very good agreement with the CDF measurement [11] $\Delta m_s = 17.77 \pm 0.10$ (stat.) $\pm$ 0.07 (syst.) ps^{-1}. The likelihood scan and amplitude scan for Δm_s are shown in Figure 4.

The B_d mixing frequency is measured to be $\Delta m_d = 0.499 \pm 0.032$ (stat.) $\pm$ 0.003 (syst.) ps^{-1} using $B_d \to D^-\pi^+$ decays, [12] consistent with the PDG [13] average value $\Delta m_d = 0.507 \pm 0.005$ ps^{-1}.

3.6 Tagged Analysis of $B_s \to J/\psi\phi$ and Prospect

While completing these proceedings, the LHCb Collaboration has reported the first preliminary results on ϕ_s from a tagged analysis of 836 ± 60 $B_s \to J/\psi\phi$ signals. No point estimate of ϕ_s is possible with this amount of data, and the results are presented as 2-dimensional confidence regions in the ($\Delta\Gamma_s$, ϕ_s) plane, which show a 1.2σ deviation from the SM expectation. The tagged analysis benefits from an excellent proper time resolution of around 50 fs. So far the analysis only uses opposite side tagging, which has an effective tagging power $\epsilon_{eff}^{OS} = (2.2 \pm 0.5)\%$. The

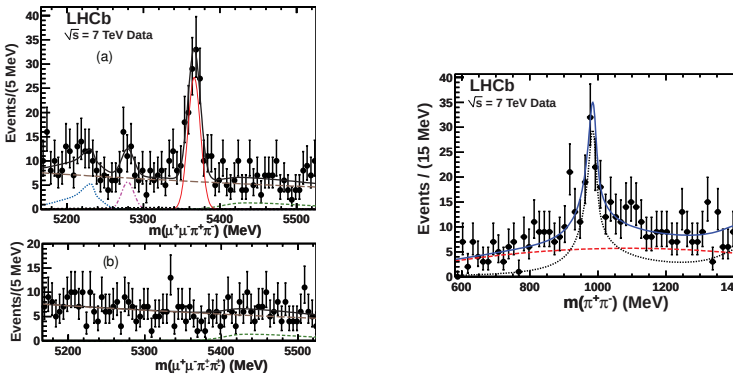

Figure 5: Left: (a) the $J/\psi\pi^+\pi^-$ mass distribution for selected candidates. Superimposed curves are the total fit (solid black), the signal (solid red), combinatorial background (long dashed brown), $B^+ \to J/\psi K^+(\pi^+)$ background (dashed green) and $B^+ \to J/\psi K^+$ background (dotted blue); (b) the same as above but for like-sign di-pion combinations. Right: the mass distribution of the $\pi^+\pi^-$ combinations. Superimposed curves are the total fit (solid blue), the interfering resonances $f_0(980)$ and $f_0(1370)$ (dotted black) and background (dashed red).

work to optimize and calibrate the same side kaon tagging is ongoing. The LHCb experiment will soon become competitive with the Tevatron experiments in measuring ϕ_s, once it collects 200 pb^{-1} of data in 2011 and include the same kaon tagging, which is expected to double the effective tagging power. LHCb aims to make the world's best measurement of ϕ_s using about 1 fb^{-1} of data due to be collected in 2011.

4 First Observation of the Decay $B_s \to J/\psi f_0(980)$

LHCb made the first observation of a new CP-odd decay $B_s \to J/\psi f_0(980)$ with about 13 standard deviations of significance, using $f_0 \to \pi^+\pi^-$. [15] Figure 5 shows the mass distributions of the $J/\psi\pi^+\pi^-$ and $\pi^+\pi^-$ combinations. The ratio to $J/\psi\phi$ production is measured as $R_{f_0/\phi} \equiv \frac{\Gamma(B_s\to J/\psi f_0, f_0\to\pi^+\pi^-)}{\Gamma(B_s\to J/\psi\phi,\phi\to K^+K^-)} = 0.252^{\pm 0.046 \pm 0.027}_{-0.032-0.033}$, consistent with the theoretical expectation. [16] The $B_s \to J/\psi f_0(\pi^+\pi^-)$ mode will be very useful for measuring the weak phase ϕ_s since it does not require any angular analysis. If the branching ratio of $f_0 \to K^+K^-$ is not too small, the interference of the $f_0(980)$ and $\phi(1020)$ contributions in $B_s \to J/\psi K^+K^-$ allows to resolve a two-fold ambiguity in the measurement of ϕ_s. [17]

5 First Observation of the Decay $B_s \to K^{*0}\bar{K}^{*0}$

LHCb made the first observation of the decay $B_s \to K^{*0}\bar{K}^{*0}$ with a 7σ significance. [18] The fit to the $K^+\pi^-K^-\pi^+$ mass distribution is shown in Figure 6. 34.0 ± 7.4 signals are found in the mass interval ± 50 MeV around the B_s mass. A preliminary measurement of the branching ratio is $BR(B_s \to K^{*0}\bar{K}^{*0}) = (1.95 \pm 0.47(stat.) \pm 0.51(syst.) \pm 0.29(f_d/f_s))\%$. This decay mode can be used to probe NP contributions in decay processes via loop diagrams. [19]

6 Conclusions and Prospects

The LHCb experiment collected about 36 pb^{-1} of data in the 2010 LHC run. Using this data sample, the experiment fully tested the mechanism for CP violation study with B decays, and produced some interesting results, including measurements of b-hadron lifetimes, measurements

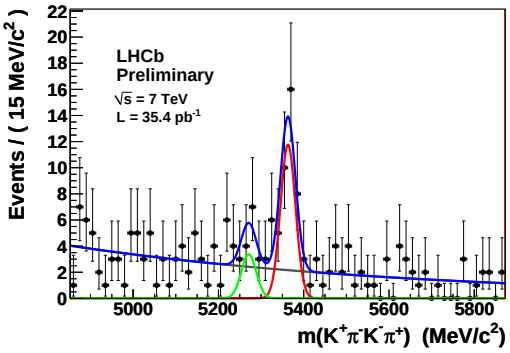

Figure 6: The $K^+\pi^-K^-\pi^+$ mass distribution for selected candidates. Superimposed curves are: the total fit (blue), Gaussian components for decays of B_s (red) and B_d (green), and an exponential component for the combinatorial background (black).

of polarization parameters in $B^0 \to J/\psi K^{*0}$ and $B_s \to J/\psi\phi$ decays, measurement of Δm_s, optimization and calibration of flavour tagging software, first observations of the decays $B_s \to J/\psi f_0(980)$ and $B_s \to K^{*0}\bar{K}^{*0}$. The LHCb experiment is ready to produce high precision results from flavour-tagged time-dependent analysis of the golden decay channel $B_s \to J/\psi\phi$ and other important channels such as $B_s \to J/\psi f_0(980)$ and $B \to hh$, using the 1 fb^{-1} of data that will be collected in 2011.

References

1. The LHCb Collaboration, LHCB-PUB-2009-029, arXiv:0912.4179.
2. The LHCb Collaboration, *Journal of Instrumentation* **3**, S08005 (2008).
3. J. Charles *et al.* (CKMfitter group), *Eur. Phys. J.* C **41**, 1 (2005).
4. The LHCb Collaboration, LHCB-CONF-2011-001.
5. The LHCb Collaboration, LHCB-CONF-2011-002.
6. The Babar Collaboration, *Phys. Rev.* D **76**, 031102 (2007).
7. The CDF Collaboration, CDF note 10206.
8. Gary J. Feldman and Robert D. Cousins, *Phys. Rev.* D **57**, 3873 (1998).
9. The LHCb Collaboration, LHCB-CONF-2011-003.
10. The LHCb Collaboration, LHCB-CONF-2011-005.
11. The CDF Collaboration, *Phys. Rev. Lett.* **97**, 242003 (2006).
12. The LHCb Collaboration, LHCB-CONF-2011-010.
13. K. Nakamura, *J. Phys.* G **37**, 075021 (2010).
14. The LHCb Collaboration, LHCB-CONF-2011-006.
15. The LHCb Collaboration, *Phys. Lett.* B **698**, 115 (2011).
16. S. Stone and L. Zhang, *Phys. Rev.* D **79**, 074024 (2009).
17. Y. Xie *et al.*, *Journal of High Energy Physics* **0909**, 074 (2009).
18. The LHCb Collaboration, LHCB-CONF-2011-019.
19. M. Ciuchini, M. Pierini, L. Silvestrini *Phys. Rev. Lett.* **100**, 031802 (2008).